Postsynaptic P/Q-type Ca^{2+} channel in Purkinje cell mediates synaptic competition and elimination in developing cerebellum

Kouichi Hashimoto[a,b,c], Mika Tsujita[d], Taisuke Miyazaki[e], Kazuo Kitamura[a,c], Maya Yamazaki[d], Hee-Sup Shin[f], Masahiko Watanabe[e], Kenji Sakimura[d], and Masanobu Kano[a,1]

[a]Department of Neurophysiology, Graduate School of Medicine, University of Tokyo, Tokyo 113-0033, Japan; [b]Department of Neurophysiology, Graduate School of Biomedical Sciences, Hiroshima University, Hiroshima 734-8551, Japan; [c]Precursory Research for Embryonic Science and Technology, Japan Science and Technology Agency, Saitama 332-0012, Japan; [d]Department of Cellular Neurobiology, Brain Research Institute, Niigata University, Niigata 951-8585, Japan; [e]Department of Anatomy, Graduate School of Medicine, Hokkaido University, Sapporo 060-8638, Japan; and [f]Center for Neural Science, Korea Institute of Science and Technology, Seoul 136-791, Korea

Edited* by Masao Ito, RIKEN Brain Science Institute, Wako, Japan, and approved May 5, 2011 (received for review January 26, 2011)

Neural circuits are initially redundant but rearranged through activity-dependent synapse elimination during postnatal development. This process is crucial for shaping mature neural circuits and for proper brain function. At birth, Purkinje cells (PCs) in the cerebellum are innervated by multiple climbing fibers (CFs) with similar synaptic strengths. During postnatal development, a single CF is selectively strengthened in each PC through synaptic competition, the strengthened single CF undergoes translocation to a PC dendrite, and massive elimination of redundant CF synapses follows. To investigate the cellular mechanisms of this activity-dependent synaptic refinement, we generated mice with PC-selective deletion of the $Ca_v2.1$ P/Q-type Ca^{2+} channel, the major voltage-dependent Ca^{2+} channel in PCs. In the PC-selective $Ca_v2.1$ knockout mice, Ca^{2+} transients induced by spontaneous CF inputs are markedly reduced in PCs in vivo. Not a single but multiple CFs were equally strengthened in each PC from postnatal day 5 (P5) to P8, multiple CFs underwent translocation to PC dendrites, and subsequent synapse elimination until around P12 was severely impaired. Thus, P/Q-type Ca^{2+} channels in postsynaptic PCs mediate synaptic competition among multiple CFs and trigger synapse elimination in developing cerebellum.

calcium channel | inferior olive | vesicular glutamate transporter 2 | Cre/loxP system | α1A subunit

In the developing nervous system, neuronal connections are initially redundant, but they are refined and become functionally mature during postnatal development by synapse elimination (1–3). It is widely believed that synapse elimination involves activity-dependent competition among surplus synaptic inputs to each postsynaptic cell (1, 4, 5). At the neuromuscular junction, effective excitation of target muscles has been shown to bias the synaptic competition in favor of the input whose synaptic efficacy is relatively stronger than others (6). However, the molecular basis for controlling synaptic competition in the central nervous system (CNS) has been largely unknown.

The cerebellar climbing fiber (CF) to the Purkinje cell (PC) synapse provides an excellent model to study synapse elimination in the CNS. Whereas most PCs in the cerebellum of adult mice receive strong excitatory inputs from single CFs (7), PCs in neonatal cerebellum are innervated by multiple CFs with similar synaptic strengths (8–10). From postnatal day 3 (P3) to P7, one CF is selectively strengthened relative to others in each PC (8–10). Then, the single "winner" CF undergoes translocation to PC dendrites (11). In parallel, redundant CFs are eliminated and most PCs become innervated by single CFs by around P17 in mice (8–10, 12). CF elimination consists of two distinct phases in mice, the early phase from P7 and the late phase from around P12 (12), which involve distinct mechanisms (9, 12). Whereas several factors crucial for the late phase of CF synapse elimination have been disclosed (13–20), mechanisms of biased strengthening of single CFs and the early phase of CF synapse elimination are unknown. Because synapse refinement critically depends on neuronal activity (1, 4, 5, 16, 21, 22), we studied whether the P/Q-type voltage-dependent Ca^{2+} channel (VDCC), the major high-threshold VDCC in PCs (23), is involved in the development of CF to PC synapses.

Results

Generation of PC-Specific $Ca_v2.1$ Knockout Mice. We previously analyzed mice lacking $Ca_v2.1$ (24), a pore-forming component of the P/Q-type VDCC (global $Ca_v2.1$ KO mice), and reported that $Ca_v2.1$ KO mice have persistent multiple-CF innervation in young adult PCs (25). Although the P/Q-type VDCC is a major high-threshold Ca^{2+} channel in PCs (23), it is also a major VDCC in presynaptic terminals that mediates transmitter release in most of the central synapses including the cerebellum (26, 27). To clarify the extent of contribution of postsynaptic P/Q-type VDCCs to developmental rearrangements of CF synapses, we generated PC-selective $Ca_v2.1$ knockout mice by using the Cre/loxP recombination system and the C57BL/6 ES cell line RENKA (28, 29). We generated the $Ca_v2.1^{lox/lox}$ ($Ca_v2.1$ floxed) mice carrying two *loxP* sequences flanking exon 4 of the $Ca_v2.1$ gene encoding the first voltage-sensor domain (Fig. 1*A*). To obtain a cerebellar PC-selective Cre recombinase expression, we used a D2CreN line ($GluD2^{+/Cre}$) whose Cre gene was expressed in PCs under the control of the GluD2 promoter (30). By intercrossing $Ca_v2.1$ floxed mice with D2CreN mice, we obtained PC-selective $Ca_v2.1$ knockout mice ($Ca_v2.1^{lox/lox}$, $GluD2^{+/Cre}$, from now on called PC-$Ca_v2.1$ KO mice) (Fig. 1 *B* and *C*). The littermates from the same breeding pairs carrying the floxed $Ca_v2.1$ gene but no Cre gene ($Ca_v2.1^{lox/lox}$, $GluD2^{+/+}$) were used as a control. Whereas conventional global $Ca_v2.1$ KO mice die before the fourth postnatal week (24), our PC-$Ca_v2.1$ KO mice grew up to adulthood and were fertile. Although expression of $Ca_v2.1$ mRNA was rich in PCs and other brain regions in control mice at P2 (Fig. S1 *A–C*) and P5 (Fig. S1 *G–I*), $Ca_v2.1$ mRNA expression was eliminated selectively from PCs in PC-$Ca_v2.1$ KO mice (Fig. S1 *D–F* and *J–L*). To check functional deletion of P/Q-type VDCCs, we recorded voltage-dependent Ca^{2+} currents from PCs in cerebellar slices at P5–P6. We found that the Ca^{2+} currents of PC-$Ca_v2.1$ KO PCs were significantly smaller than those of control PCs (Fig. 1*D*). Then, we additively bath-applied the N-type VDCC blocker ω-conotoxin GVIA (ω-CTX, 3 μM),

Author contributions: K.H., M.W., K.S., and M.K. designed research; K.H., M.T., T.M., K.K., and M.Y. performed research; M.T., H.-S.S., and K.S. contributed new reagents/analytic tools; K.H., M.T., T.M., K.K., and M.Y. analyzed data; and K.H., M.W., and M.K. wrote the paper.

The authors declare no conflict of interest.

*This Direct Submission article had a prearranged editor.

[1]To whom correspondence should be addressed. E-mail: mkano-tky@m.u-tokyo.ac.jp.

This article contains supporting information online at www.pnas.org/lookup/suppl/doi:10.1073/pnas.1101488108/-/DCSupplemental.

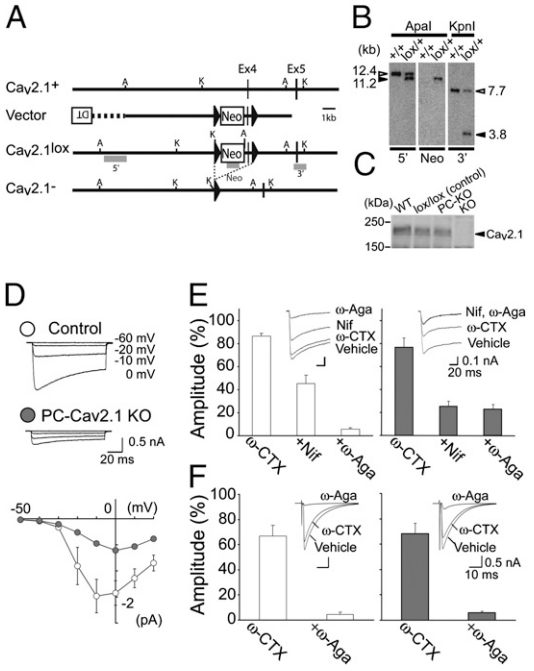

Fig. 1. Generation of PC-specific $Ca_v2.1$ knockout mice. (*A*) Schematic representations of $Ca_v2.1$ cDNA, $Ca_v2.1$ genomic DNA ($Ca_v2.1^+$), targeting vector, targeted genome ($Ca_v2.1^{lox}$), and Cre-mediated deleted genome ($Ca_v2.1^-$). Solid triangles indicate *loxP* sequences. Shaded bars indicate the probes (5′, Neo, and 3′) for Southern blot analysis. A, ApaI; K, KpnI. (*B*) Southern blot analysis of genomic DNA prepared from the wild-type ($^{+/+}$) and $Ca_v2.1^{lox/+}$ ES cells. (*Left*) ApaI-digested DNA hybridized with a 5′ probe: 12.4 kb for wild-type and 11.2 kb for floxed allele. (*Middle*) ApaI-digested DNA hybridized with a Neo probe: 11.2 kb for floxed allele. (*Right*) KpnI-digested DNA hybridized with a 3′ probe: 7.7 kb for wild-type and 3.8 kb for floxed allele. (*C*) Western blot analysis of the homogenates from the cerebellum of $Ca_v2.1^{+/+}$ (WT), control (lox/lox), PC-$Ca_v2.1$ KO (PC-KO), and global $Ca_v2.1$ KO (KO) mice at P20. Proteins loaded in each lane are 50 μg. (*D*) PC-selective deletion of P/Q-type VDCCs in PC-$Ca_v2.1$ KO mice. (*Upper*) Specimen records of Ca^{2+} currents elicited by 100 ms depolarization from V_h = −60 mV to −20, −10, and 0 mV in PCs at P5. (*Lower*) Current–voltage relationship in control (open symbols, n = 6) and PC-$Ca_v2.1$ KO (solid symbols, n = 6) mice at P5. Peak amplitudes are plotted against the voltage steps. (*E*) Pharmacology of Ca^{2+} currents in control (*Left*, n = 8) and PC-$Ca_v2.1$ KO (*Right*, n = 8) mice. Averaged amplitudes are measured from 10 ms at the end of voltage step (90–100 ms). (*Insets*) Specimen records of Ca^{2+} currents. (*F*) Pharmacology of CF-EPSCs elicited in control (*Left*, n = 6) and PC-$Ca_v2.1$ KO (*Right*, n = 7) mice. (*Insets*) Specimen records of CF-EPSCs.

the L-type VDCC blocker nifedipine (Nif, 10 μM), and the P/Q-type VDCC blocker ω-agatoxin IVA (ω-Aga, 0.4 μM) while monitoring the current through VDCCs (depolarization from −60 to −10 mV) every 30 s by using Ba^{2+} as charge carrier. We demonstrate that the component mediated by the P/Q-type VDCC was absent in PC-$Ca_v2.1$ KO PCs (Fig. 1*E*), indicating that the functional P/Q-type VDCC was completely deleted by P5 from PC-$Ca_v2.1$ KO PCs. In marked contrast to the postsynaptic change, the P/Q channel contributed to the same extent to CF to PC synaptic transmission in PC-$Ca_v2.1$ KO and control mice (Fig. 1*F*). These results demonstrate that the P/Q channel at the presynaptic terminal is intact and functions normally in PC-$Ca_v2.1$ KO mice.

Reduced CF-Induced Ca^{2+} Transients in PCs in Vivo of PC-$Ca_v2.1$ KO Mice. We examined how PC-selective deletion of the P/Q-type VDCC affects excitatory postsynaptic potentials (EPSPs), spike activity, and Ca^{2+} transients by CF inputs in PCs in vivo. Under isoflurane anesthesia, we performed simultaneous whole-cell recordings and two-photon Ca^{2+} imaging from PCs in vivo in control and PC-$Ca_v2.1$ KO mice at P7–P11 by using the "shadow-patching" technique (31). Spontaneous simple spike activity was suppressed by injecting hyperpolarizing currents, and responses caused by spontaneous CF inputs were recorded at ∼ −60 mV. In control mice, PCs exhibited irregular burst firing responses that were composed of large EPSPs and multiple spikes, which are thought to be generated by spontaneous CF inputs (Fig. 2*A*). These burst firings occasionally appeared in train. Each train of burst firing induced a clear Ca^{2+} transient in the soma and dendrites of PCs and resulted in prominent elevation of intracellular Ca^{2+} levels for several seconds. In PC-$Ca_v2.1$ KO mice, PCs also exhibited irregular burst firings and occasional trains of burst firing (Fig. 2*B*). Although average firing rates of burst firing were not significantly different between control and PC-$Ca_v2.1$ KO mice (Fig. 2*C*, P = 0.14), magnitudes of Ca^{2+} influx were significantly smaller in PC-$Ca_v2.1$ KO mice compared with control mice (Fig. 2*D*). As a consequence of reduced Ca^{2+} transients associated with each burst firing, elevation of intracellular Ca^{2+} levels caused by occasional burst trains was significantly smaller in PC-$Ca_v2.1$ KO mice than in control mice. These results demonstrate that Ca^{2+} transients induced by spontaneous CF inputs are markedly reduced in PCs of PC-$Ca_v2.1$ KO mice in vivo.

Impaired CF Synapse Elimination Until Around P12 in PC-$Ca_v2.1$ KO Mice. We examined the CF innervation pattern in young adult PC-$Ca_v2.1$ KO mice by using whole-cell recordings from PCs in acute cerebellar slices (25). Compared with control mice, the regression of surplus CFs was severely impaired in PC-$Ca_v2.1$ KO mice (Fig. 3 *A* and *B*) to the same extent as that observed in global $Ca_v2.1$ KO mice (25). Basic properties of CF-mediated excitatory postsynaptic currents (CF-EPSCs) were similar between control and PC-$Ca_v2.1$ KO mice, although the 10–90% rise time and decay time constants were longer in PC-$Ca_v2.1$ KO mice (Table S1). We then examined at which stage of postnatal development the abnormality of synapse elimination becomes

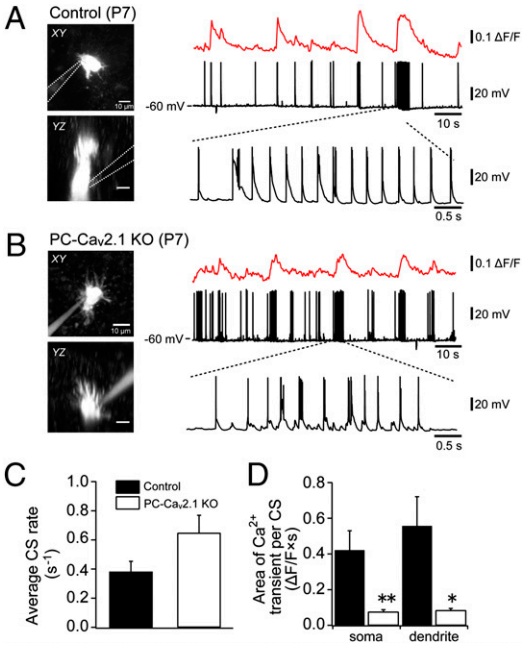

Fig. 2. Reduction in CF-mediated Ca^{2+} transients in PCs of PC-$Ca_v2.1$ KO mice. (*A* and *B*) Simultaneous whole-cell recordings and two-photon Ca^{2+} imaging from PCs of control (*A*) and PC-$Ca_v2.1$ KO (*B*) mice in vivo. (*Left*) Horizontal (*Upper*) and parasaggital (*Lower*) projection images of recorded PCs at P7. (*Right*) Somatic Ca^{2+} transients (*Top*) and membrane potential (*Middle*) were recorded simultaneously. Note that trains of burst firing were often observed (*Bottom*). (*C*) Average firing rate of burst firing. (*D*) Somatic and dendritic Ca^{2+} elevation evoked by each train of burst firing was quantified as (area of Ca^{2+} transients)/(number of burst firings in train). *P < 0.002; **P < 0.0001.

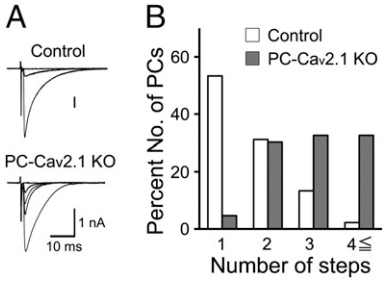

Fig. 3. Persistent multiple CF innervations of PCs in young adult PC-$Ca_v2.1$ KO mice. (*A*) Specimen records of CF-EPSCs in control (P19; V_h = −20 mV) and PC-$Ca_v2.1$ KO (P20; V_h = −20mV) mice. (*B*) Frequency distribution histogram for the number of CFs innervating each PC in control (open columns, n = 45) and PC-$Ca_v2.1$ KO (shaded columns, n = 43) mice at P19–P31.

obvious in PC-$Ca_v2.1$ KO mice. At P4–P6, the majority of PCs were innervated by four or more CFs in both PC-$Ca_v2.1$ KO and control mice (Fig. 4*A* and Fig. S2*A*). The number of CFs innervating each PC was identical between control [9.1 ± 0.5 (mean ± SEM), n = 48 PCs] and PC-$Ca_v2.1$ KO (10.4 ± 0.7, 38 PCs) (P = 0.227). Then, during the following postnatal period, the number of CFs progressively decreased in control PCs (Fig. 4 *B–E* and Fig. S2 *B–E*). In marked contrast, distributions of PCs remained almost unchanged until P12 in PC-$Ca_v2.1$ KO PCs (Fig. 4 *B* and *C* and Fig. S2 *B* and *C*). The number of CFs innervating each PC decreased at P12–P15 (Fig. 4*D*), but elimination did not proceed thereafter (Fig. 4 *D* and *E* and Fig. S2 *D* and *E*). When the percentage of PCs innervated by four or more CFs was plotted against postnatal day, this value progressively decreased from P6 to P12 in control mice (Fig. 4*F*). In contrast, the percentage remained high until around P12 in PC-$Ca_v2.1$ KO mice (Fig. 4*F*). Then, the value decreased to ∼30%, but did not reach the level of control mice (Fig. 4*F*). These results suggest that initial CF innervation is normal, but the following elimination process from around P7 to P12 is severely impaired in PC-$Ca_v2.1$ KO mice.

Impaired Functional Differentiation of Multiple CF Inputs in PC-$Ca_v2.1$ KO PCs. Next, we examined whether selective strengthening of a single CF in each PC during the first postnatal week is affected in PC-$Ca_v2.1$ KO mice. To quantify functional differentiation of multiple CF inputs, we calculated the parameter (disparity index) used in our previous study (Fig. 5*A*) (9). In control mice, the disparity index increased from P5 to P7 and reached a plateau. Because an increase in the disparity index indicates the increase in the difference among the amplitudes of multiple CF-EPSCs, this evidence implies that CF-EPSC amplitudes of multiple CFs are initially similar but EPSCs from a single CF undergo biased strengthening until P7 in control PCs (9). In contrast, the robust increase in the disparity index until around P7 was not seen in PC-$Ca_v2.1$ KO PCs (Fig. 5*A*). This result indicates that biased strengthening of single CFs from P5 to P7 is severely impaired in PC-$Ca_v2.1$ KO PCs.

We then measured whether the absolute EPSC amplitude changes in each PC during postnatal development (Fig. 5*B*). In both control and PC-$Ca_v2.1$ KO PCs, the total amplitude of CF-EPSCs increased about fourfold from P5 to P8 with no significant difference between the two mouse strains (Fig. 5*B*), indicating that developmental increase in the total amount of CF synaptic input on each PC is normal in $Ca_v2.1$ KO mice. This result suggests that the number of CF synapses on each PC increases normally in PC-$Ca_v2.1$ KO mice, because each CF forms multiple synaptic contacts on PCs and the number of CF terminals is thought to be proportional to CF-EPSC amplitude. We measured the density of CF terminals around the PC soma at P10 by counting large synaptic boutons immunopositive for vesicular glutamate transporter 2 (VGluT2), a marker for CF terminals (25). As expected from the electrophysiological data, the density was not different between control and PC-$Ca_v2.1$ KO PCs (Fig. S3).

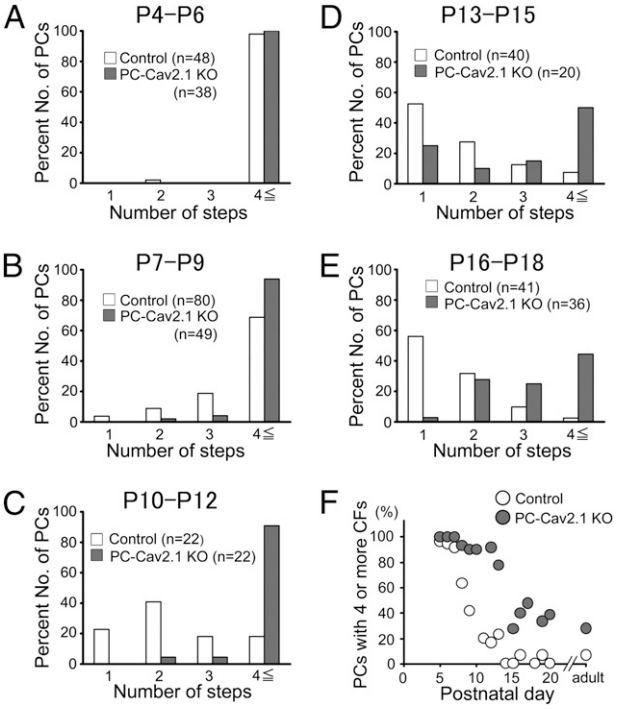

Fig. 4. Impairment of CF synapse elimination during postnatal development in PC-$Ca_v2.1$ KO mice. (*A–E*) Frequency distribution histogram for the number of discrete CF-EPSCs for control and PC-$Ca_v2.1$ KO mice illustrated similarly to Fig. 3*B*. There is no significant difference in the frequency distribution in *A* between control and PC-$Ca_v2.1$ KO mice (P = 0.871; Mann–Whitney U test). In contrast, frequency distributions for *B–E* are significantly different between control and PC-$Ca_v2.1$ KO mice (*B*, P = 0.023; *C–E*, P < 0.001). (*F*) Developmental changes in the fraction of PCs innervated by four or more CFs.

We then calculated the fractions of individual CF-EPSC amplitudes relative to the total CF-EPSC amplitude in each PC (Fig. 5 *C* and *D*). In control mice, the fraction of the largest CF-EPSC increased from P5 to P8, but those of the second to fourth largest CF-EPSCs remained unchanged or gradually decreased (Fig. 5*C*). In contrast, the fractions of multiple CF-EPSCs remained almost unchanged from P5 to P8 in PC-$Ca_v2.1$ KO mice (Fig. 5*D*). Thus, a single CF input to each PC gains biased strengthening of synaptic efficacy in control mice, whereas multiple CF inputs are almost equally strengthened in PC-$Ca_v2.1$ KO mice. These results indicate that strengthening of total CF synaptic efficacy does not require P/Q-type VDCCs in PCs, whereas biasing the synaptic competition toward single CF inputs is critically dependent on P/Q-type VDCCs in PCs.

Our recent study demonstrates that GluD2 is weakly expressed in GABAergic interneurons in the molecular layer from early postnatal development (30). It is therefore possible that Cre recombinase is expressed also in molecular layer interneurons in GluD2$^{+/Cre}$ mice and that the P/Q-type VDCC is deleted in interneurons of PC-$Ca_v2.1$ KO mice. We checked whether GABAergic inputs to PCs were affected in PC-$Ca_v2.1$ KO mice at P6–P7 and P10, the stages at which CF synapse development was severely impaired in PC-$Ca_v2.1$ KO mice. We found no abnormality in the amplitude and frequency of spontaneous GABAergic synaptic currents in PCs of PC-$Ca_v2.1$ KO mice (Table S2), indicating that activity of GABAergic synaptic inputs to PCs is similar between control and PC-$Ca_v2.1$ KO mice. However, when inhibitory postsynaptic currents (IPSCs) evoked by stimulating axons of the molecular layer interneurons were examined at P12–P13, the P/Q-type VDCC blocker ω-agatoxin IVA (0.4 μM) reduced the amplitude to 9 ± 4% (n = 5 PCs) in control mice and to 69 ± 17% (n = 7 PCs) in PC-$Ca_v2.1$ KO mice. This result indicates that the P/Q-type VDCC is partially

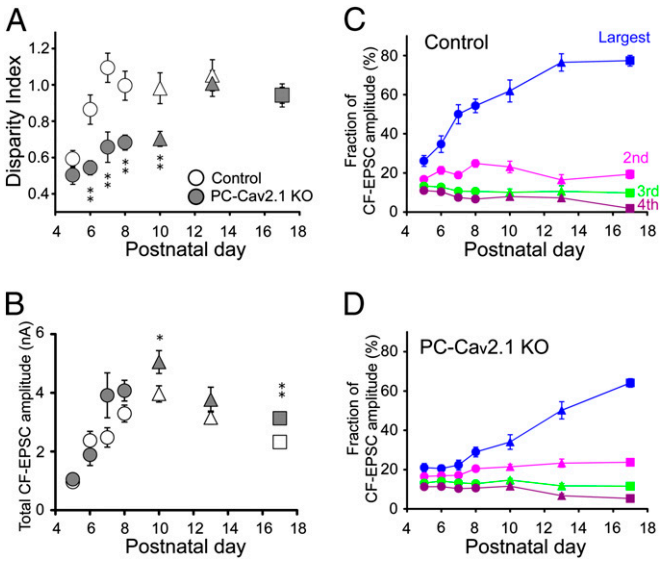

Fig. 5. Impairment of postnatal development of CFs in PC-$Ca_v2.1$ KO mice. (*A*) Developmental changes in the disparity index. The numbers of PCs for each data point are 19–42 for control and 9–62 for PC-$Ca_v2.1$ KO mice. Data for P9–P11 and P12–P14 are pooled and indicated with triangles. Data for P15–P21 are pooled and indicated with boxes. (*B*) Postnatal changes in the total amplitudes of CF-EPSCs (at V_h = −20 mV) elicited in each PC. Plots include the data for mono-innervating CFs. The numbers of PCs for each data point are 19–77 for control and 9–70 for PC-$Ca_v2.1$ KO mice. (*C* and *D*) Postnatal changes in the fractions of the largest (blue), second (pink), third (green), and fourth (violet) EPSC amplitudes relative to the total CF-EPSC amplitude in control (*C*) and PC-$Ca_v2.1$ KO (*D*) PCs.

deleted from presynaptic terminals of molecular layer interneurons at P12–P13. The deletion of the P/Q-type VDCC may lead to the decrease in GABAergic inhibition in the young adult stage, as observed in slices from global $Ca_v2.1$ KO cerebellum that were cultured for at least 3 wk (32). However, because we detected no change in spontaneous IPSCs at P6–P7 and P10 between PC-$Ca_v2.1$ KO and control mice (Table S2), the defects in CF synapse development in PC-$Ca_v2.1$ KO mice from P5 to around P10 are considered most likely to result from the lack of P/Q-type VDCCs in PCs.

Impaired CF Synapse Development in Global $Ca_v2.1$ KO Mice. To clarify the possible contribution of P/Q-type VDCCs expressed in cells other than PCs, we examined the development of CF synapses in global P/Q-type VDCC knockout mice (global $Ca_v2.1$ KO mice). At P4–P6, PCs of global $Ca_v2.1$ KO mice were innervated by about the same number of CFs as those of their wild-type littermates (Fig. S4*A*), but CF synapse elimination did not proceed from P7 to P12 (Fig. S4 *B–E*). The percentage of PCs innervated by four or more CFs decreased steeply from P6 to P11 in control mice (Fig. S4*F*), whereas the value was almost unchanged during the same postnatal period in global $Ca_v2.1$ KO mice (Fig. S4*F*). We also found that the robust increase in the disparity index from P5 to P7 was absent in global $Ca_v2.1$ KO mice (Fig. S5*A*), although developmental changes in total CF-EPSC amplitude were normal (Fig. S5*B*). The fractions of multiple CF-EPSCs remained almost unchanged from P5 to P8 in global $Ca_v2.1$ KO mice (Fig. S5*D*), whereas the fraction of the largest CF-EPSC selectively became larger in wild-type mice (Fig. S5*C*). Taken together, these results demonstrate that biased strengthening of single CF inputs during the first postnatal week and the subsequent elimination of surplus CFs until around P12 are severely impaired to the same extent in global $Ca_v2.1$ KO and PC-$Ca_v2.1$ KO mice. Therefore, the lack of P/Q-type VDCCs in cells other than PCs seems to have no additive effect on the impaired refinement of CF-PC synapses until around P12.

Translocation of Multiple CFs to PC Dendrites in PC-$Ca_v2.1$ KO Mice. To examine CF innervation patterns morphologically, we performed triple fluorescent labeling of cerebella at P12 and P16 for calbindin (PC marker, blue), VGluT2 (CF terminal marker, green) and anterograde tracer dextran Alexa 594 (DA-594, red) (Fig. 6). We analyzed the PCs that were innervated by tracer-labeled predominant CFs to specify the pattern (mono-innervation or multiple innervation) and the site (soma or dendrite) of CF innervation. In control mice at P12, predominant CFs double labeled for DA-594 and VGluT2 innervated both somata and proximal shaft dendrites of PCs, whereas terminals of surplus CFs labeled for VGluT2 alone were virtually confined to the soma (Fig. 6*A*). At P16, predominant CFs further extended along dendrites with an increased number of their branches, whereas they lost their terminals on the soma or innervated apical portions of the soma (Fig. 6*B*). At this stage, surplus CF terminals were much less frequent than at P12 (Fig. 6*B*). In PC-$Ca_v2.1$ KO mice, surplus CF terminals were far more numerous than in control mice at both P12 and P16 (Fig. 6 *C* and *D*). These surplus CF terminals were distributed over not only the soma but also the proximal shaft dendrites of PCs (Fig. 6 *C* and *D*), thus indicating dendritic translocation of multiple CFs in PCs of PC-$Ca_v2.1$ KO mice.

Then we quantitatively evaluated the pattern and site of CF innervation on the basis of our morphological data. We classified PCs into three groups: mono-innervation (*mono*), multiple innervation with surplus CF innervation confined to the soma (*multisoma*), and multiple innervation with surplus CF innervation extending to dendrites (*multidendrite*). By triple immunofluorescence for calbindin, VGluT2, and glial marker glial high affinity glutamate transporter (GLT-1), we found that ~80% of VGluT2-positive CF terminals had direct contacts to the apical half of PC somata in control and PC-$Ca_v2.1$ KO mice (Fig. S6 *A*, *C*, *E*, and *F*). In contrast, more than half of the VGluT2-positive terminals in the basal half of PC somata were apparently apart from the somatic membrane with intervening glial sheets between the pre- and postsynaptic elements (Fig. S6 *B* and *D–F* and *SI Results*). Such VGluT2-positive terminals around the basal half of PC somata were often in contact with dendritic profiles of unidentified neurons. Therefore, we judged the PCs whose apical half of the soma was contacted by terminals of surplus CFs as the multisoma type.

In control mice, percentages of the mono, multisoma, and multidendrite types were 36%, 60%, and 5% (27, 45, and 3 of 75 PCs), respectively, at P12 and 81%, 19%, and 0% (47, 11, and 0 of 58 PCs) at P16 (Fig. 6 *E* and *F*, open columns). In PC-$Ca_v2.1$ KO mice, most PCs are multiply innervated; percentages of the mono, multisoma, and multidendrite types were 2%, 53%, and 45% (27, 49, and 41 of 92 PCs), respectively, at P12 and 24%, 36%, and 40% (18, 28, and 31 of 77 PCs) at P16 (Fig. 6 *E* and *F*, shaded columns). These results from control mice conform to our previous study reporting that single winner CFs translocate to PC dendrites, whereas "loser" CFs remain around the somata and are subsequently eliminated (11). The results from PC-$Ca_v2.1$ KO mice demonstrate that the lack of P/Q-type VDCCs permits multiple CFs to translocate to dendrites and impairs elimination of CF synapses from the soma.

Discussion

We found that PC-$Ca_v2.1$ KO mice had severe defects in biased strengthening of single CF inputs from P5 to P7, subsequent dendritic translocation of the strengthened CF, and the early phase of CF synapse elimination until around P12. We verified that a voltage-dependent Ca^{2+} current component mediated by a P/Q-type VDCC was completely eliminated in PCs (Fig. 1 *D* and *E*), whereas presynaptic P/Q-type VDCCs functioned normally at CF-PC synapses of PC-$Ca_v2.1$ KO mice (Fig. 1*F*). Furthermore, the amplitude and frequency of spontaneous GABAergic synaptic currents were normal in PCs of PC-$Ca_v2.1$ KO mice (Table S2). These results strongly suggest that P/Q-type VDCCs in postsynaptic PCs are essential for the refinement of CF synapses during the first 12 d of mouse postnatal development.

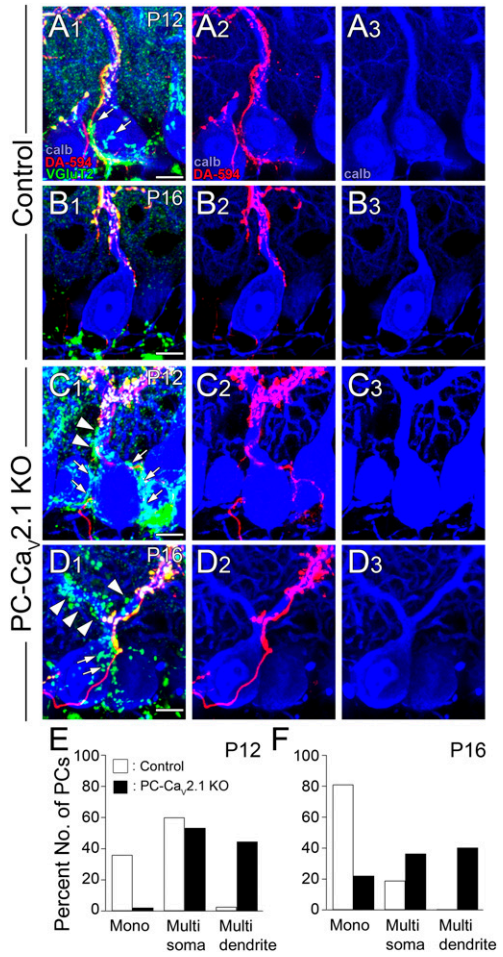

Fig. 6. Dendritic translocation of multiple CFs and persistent somatic CF innervation in PC-Ca_v2.1 KO mice. (*A–D*) Triple fluorescent labeling for calbindin (blue), VGluT2 (green), and anterograde tracer dextran Alexa-594 (DA-594, red) in control (*A* and *B*) and PC-Ca_v2.1 KO (*C* and *D*) mice at P12 (*A* and *C*) and P16 (*B* and *D*). Arrows and arrowheads indicate tracer-unlabeled/VGluT2-positive CF terminals on the soma and the dendrite, respectively, for a given PC. (*E* and *F*) Classification of anatomically identified CF innervation at P12 (*E*) and P16 (*F*). PCs innervated solely by tracer-labeled CFs are classified as mono-innervation (mono), whereas those innervated by both tracer-labeled and tracer-unlabeled CFs are classified as multiple innervation (multi). Multiply innervated PCs are further classified on the basis of whether tracer-unlabeled CFs are confined to the soma (multisoma) or extend to dendrites (multidendrite). (Scale bar, 10 μm.)

We found that CF synapse elimination starting at around P7 was severely impaired in PC-Ca_v2.1 KO mice (Figs. 3 and 4). The process of CF synapse elimination is shown to consist of the early and late phases (13, 33, 34). In mice, the early phase ranges from P7 to around P11, and the late phase from around P12 to P17 (35). In the present study, we found that the majority of PCs were innervated by four or more CFs both in control and in PC-Ca_v2.1 KO mice at P4–P6. In PC-Ca_v2.1 KO mice, the subsequent elimination of surplus CFs did not proceed properly (Fig. 4). These results suggest that initial synapse formation by multiple CFs is almost normal, but the following elimination process from P7 is severely impaired in PC-Ca_v2.1 KO mice. This developmental period is before the robust formation of parallel fiber (PF) synapses (36–39). The impairment of CF synapse elimination becomes evident clearly earlier than that of the knockout mice deficient in the mGluR1 signaling cascade in which the late phase is selectively impaired (17–20).

In PC-Ca_v2.1 KO mice, the rapid increase in the disparity index during the first postnatal week was severely impaired (Fig. 5*A*) and the fractions of the amplitudes of individual CF-EPSCs relative to the total CF-EPSC amplitude were almost constant (Fig. 5*D*), indicating the impairment of biased strengthening of single CF inputs. Importantly, the total CF-EPSC amplitude in individual PCs increased by about fourfold from P5 to P8 in PC-Ca_v2.1 KO mice similarly to the control mice (Fig. 5*B*). The density of the CF terminal on the soma of each PC is similar between control and PC-Ca_v2.1 KO PCs (Fig. S3). These results clearly indicate that the developmental increase in the number of CF terminals is normal in the Ca_v2.1-deficient mice. Therefore, we conclude that strengthening of total CF synaptic efficacy and biasing the synaptic competition toward single CF inputs are based on different mechanisms. Molecular bases for these developmental changes are currently unknown. However, it is likely that developmental change in the amount of resource necessary for maintaining synaptic efficacy and competition for such a resource by multiple CFs are two important factors (3, 40). As the amount of resource increases with postnatal development, the total CF synaptic efficacy becomes larger. This process itself is independent of P/Q-type VDCCs in PCs, but the assignment of the resource to given CFs may be dependent on P/Q-type VDCC-mediated activity. Stronger CFs can activate postsynaptic P/Q-type VDCCs more effectively and may gain more resource than weaker CFs. This competition may eventually result in selective strengthening of a single winner CF and weakening of the rest of the CFs in each PC.

After selective strengthening of a single CF during the first postnatal week, only the winner CF undergoes translocation to PC dendrites, which starts at around P9 in control mice (11). By marked contrast, our morphological data clearly demonstrate that more than one CF form synaptic contacts on PC dendrites at P12 and P16 in PC-Ca_v2.1 KO mice (Fig. 6), indicating that multiple CFs undergo dendritic translocation in PC-Ca_v2.1 KO mice. Because the disparity between the strongest CF and other CFs is small at P9 in PC-Ca_v2.1 KO and global Ca_v2.1 KO PCs, it is likely that the strongest CF cannot suppress dendritic translocation of other weaker CFs. As a result, weaker CFs may compete with the strongest CF for gaining innervation territories in dendrites in the Ca_v2.1-deficient PCs. Another possibility would be that CF inputs that gave rise to a certain level of Ca^{2+} elevation could translocate to the dendritic shafts of PCs, and multiple CFs in PC-Cav2.1 KO mice might meet this criterion.

The phenotypes of Ca_v2.1 KO mice are not likely to reflect the slowing of development. If the delayed development is the major cause, synaptic organization of PCs of young adult Ca_v2.1 KO mice should resemble that of control mice at a certain stage of postnatal development. However, PCs of Ca_v2.1 KO mice have abnormalities that are not seen in developing PCs of control mice, including hyperspiny transformation and dendritic translocation of multiple CFs (25). Moreover, the developmental increase in total CF-EPSC amplitude (Fig. 5*B* and Fig. S5*B*) and the initiation of CF translocation (Fig. 6*C*) appear normal. Therefore, we conclude that the defects in Ca_v2.1 KO mice result from the impairment of specific processes of CF synapse elimination rather than the delay of development.

Although several factors crucial for the late phase of CF synapse elimination have been elucidated (12, 16–19, 41–44), the molecular bases for the functional differentiation, subsequent dendritic translocation, and the early phase of CF synapse elimination were unclear. The present study demonstrates unequivocally that the P/Q-type VDCC in PCs is crucial for such rearrangements of CF synapses during the first 12 d of postnatal development. Because PF synapses are immature during this developmental stage, activation of the P/Q-type VDCC in PCs should be caused by CF inputs. Recently, long-term potentiation (LTP) and depression (LTD) of CF synapses were reported in PCs of neonatal rodents (8, 45). Interestingly, LTP occurs exclusively at large CF inputs that produce significant Ca^{2+} transients in PCs, whereas LTD is induced at small CF inputs that are not associated with Ca^{2+} transients (8). LTP/LTD of CF synapses may contribute to selective strengthening/weakening of CF inputs during the first postnatal week, which may determine

the single winner CF that will remain throughout life and loser CFs that will eventually be eliminated.

Materials and Methods

Animals. All animal experiments were carried out in accordance with the guidelines laid down by the animal welfare committees of Niigata University, Hokkaido University, Hiroshima University, and University of Tokyo. We generated the $Ca_v2.1^{lox/lox}$ ($Ca_v2.1$ floxed) mice carrying two loxP sequences flanking exon 4 of the $Ca_v2.1$ gene encoding the first voltage-sensor domain (Fig. 1*A*). Details of the procedures to generate $Ca_v2.1^{lox/lox}$ mice are described in *SI Materials and Methods*.

Electrophysiology. Mice aged 5–31 d postnatally were decapitated following CO_2 anesthesia, and brains were rapidly removed and placed in chilled external solution (0–4 °C) containing 125 mM NaCl, 2.5 mM KCl, 2 mM $CaCl_2$, 1 mM $MgSO_4$, 1.25 mM NaH_2PO_4, 26 mM $NaHCO_3$, and 20 mM glucose, bubbled with 95% O_2 and 5% CO_2 (pH 7.4). Parasagittal cerebellar slices (250 μm thick) were prepared by using a vibratome slicer (Leica). Whole-cell recordings were made from visually identified PCs using an upright microscope (Olympus) at 32 °C. Compositions of the pipette solutions and protocols of stimulation and recording are described in *SI Materials and Methods*. Whole-cell recordings and two-photon Ca^{2+} imaging from PCs in anesthetized mice were performed as described (31). The details are described in *SI Materials and Methods*.

Morphological Analysis. Dextran Alexa 594 (DA-594; Invitrogen) was injected into the inferior olive to label CFs as described (46). After 4 d of survival, mice were fixed by transcardial perfusion and parasagittal cerebellar sections (50 μm in thickness) were cut (11, 15, 25). Sections were either double-immunofluorescent labeled for calbindin and VGluT2 or triple-immunofluorescent labeled for calbindin, VGluT2, and GLT-1. Details of the procedures for immunohistochemistry and in situ hybridization are described *SI Materials and Methods*.

ACKNOWLEDGMENTS. We thank M. Abe, R. Natsume, and E. Kushiya for preparation of conditional knockout mice and T. Tabata for helpful discussion. This work was supported by Grants-in-Aid for Scientific Research [17023021, 21220006, and 21650094 (to M.K.); 19100005 (to M.W.); 21300118 (to K.S.); and 22300125 (to K.H.)], the Strategic Research Program for Brain Sciences (Development of Biomarker Candidates for Social Behavior), and the Global Centers of Excellence Program (Integrative Life Science Based on the Study of Biosignaling Mechanisms) from Ministry of Education, Culture, Sports, Science and Technology, Japan. H.-S.S. was supported by a grant from the leader science support program of the Korean government.

1. Lichtman JW, Colman H (2000) Synapse elimination and indelible memory. *Neuron* 25: 269–278.
2. Purves D, Lichtman JW (1980) Elimination of synapses in the developing nervous system. *Science* 210:153–157.
3. Sanes JR, Lichtman JW (1999) Development of the vertebrate neuromuscular junction. *Annu Rev Neurosci* 22:389–442.
4. Hensch TK (2004) Critical period regulation. *Annu Rev Neurosci* 27:549–579.
5. Katz LC, Shatz CJ (1996) Synaptic activity and the construction of cortical circuits. *Science* 274:1133–1138.
6. Buffelli M, et al. (2003) Genetic evidence that relative synaptic efficacy biases the outcome of synaptic competition. *Nature* 424:430–434.
7. Ito M (1984) *The Cerebellum and Neural Control* (Raven, New York).
8. Bosman LW, Takechi H, Hartmann J, Eilers J, Konnerth A (2008) Homosynaptic long-term synaptic potentiation of the "winner" climbing fiber synapse in developing Purkinje cells. *J Neurosci* 28:798–807.
9. Hashimoto K, Kano M (2003) Functional differentiation of multiple climbing fiber inputs during synapse elimination in the developing cerebellum. *Neuron* 38:785–796.
10. Hashimoto K, Kano M (2005) Postnatal development and synapse elimination of climbing fiber to Purkinje cell projection in the cerebellum. *Neurosci Res* 53:221–228.
11. Hashimoto K, Ichikawa R, Kitamura K, Watanabe M, Kano M (2009) Translocation of a "winner" climbing fiber to the Purkinje cell dendrite and subsequent elimination of "losers" from the soma in developing cerebellum. *Neuron* 63:106–118.
12. Kano M, Hashimoto K (2009) Synapse elimination in the central nervous system. *Curr Opin Neurobiol* 19:154–161.
13. Crepel F (1982) Regression of functional synapses in the immature mammalian cerebellum. *Trends Neurosci* 5:266–269.
14. Hashimoto K, et al. (2001) Roles of glutamate receptor δ2 subunit (GluRδ 2) and metabotropic glutamate receptor subtype 1 (mGluR1) in climbing fiber synapse elimination during postnatal cerebellar development. *J Neurosci* 21:9701–9712.
15. Ichikawa R, et al. (2002) Distal extension of climbing fiber territory and multiple innervation caused by aberrant wiring to adjacent spiny branchlets in cerebellar Purkinje cells lacking glutamate receptor δ2. *J Neurosci* 22:8487–8503.
16. Kakizawa S, Yamasaki M, Watanabe M, Kano M (2000) Critical period for activity-dependent synapse elimination in developing cerebellum. *J Neurosci* 20:4954–4961.
17. Kano M, et al. (1995) Impaired synapse elimination during cerebellar development in PKC γ mutant mice. *Cell* 83:1223–1231.
18. Kano M, et al. (1997) Persistent multiple climbing fiber innervation of cerebellar Purkinje cells in mice lacking mGluR1. *Neuron* 18:71–79.
19. Kano M, et al. (1998) Phospholipase cbeta4 is specifically involved in climbing fiber synapse elimination in the developing cerebellum. *Proc Natl Acad Sci USA* 95: 15724–15729.
20. Offermanns S, et al. (1997) Impaired motor coordination and persistent multiple climbing fiber innervation of cerebellar Purkinje cells in mice lacking Galphaq. *Proc Natl Acad Sci USA* 94:14089–14094.
21. Lorenzetto E, et al. (2009) Genetic perturbation of postsynaptic activity regulates synapse elimination in developing cerebellum. *Proc Natl Acad Sci USA* 106: 16475–16480.
22. Rabacchi S, Bailly Y, Delhaye-Bouchaud N, Mariani J (1992) Involvement of the *N*-methyl D-aspartate (NMDA) receptor in synapse elimination during cerebellar development. *Science* 256:1823–1825.
23. Usowicz MM, Sugimori M, Cherksey B, Llinás R (1992) P-type calcium channels in the somata and dendrites of adult cerebellar Purkinje cells. *Neuron* 9:1185–1199.
24. Jun K, et al. (1999) Ablation of P/Q-type Ca^{2+} channel currents, altered synaptic transmission, and progressive ataxia in mice lacking the α_{1A}-subunit. *Proc Natl Acad Sci USA* 96:15245–15250.
25. Miyazaki T, Hashimoto K, Shin HS, Kano M, Watanabe M (2004) P/Q-type Ca^{2+} channel α1A regulates synaptic competition on developing cerebellar Purkinje cells. *J Neurosci* 24:1734–1743.
26. Mintz IM, Sabatini BL, Regehr WG (1995) Calcium control of transmitter release at a cerebellar synapse. *Neuron* 15:675–688.
27. Mintz IM, et al. (1992) P-type calcium channels blocked by the spider toxin omega-Aga-IVA. *Nature* 355:827–829.
28. Fukaya M, et al. (2006) Abundant distribution of TARP γ-8 in synaptic and extrasynaptic surface of hippocampal neurons and its major role in AMPA receptor expression on spines and dendrites. *Eur J Neurosci* 24:2177–2190.
29. Mishina M, Sakimura K (2007) Conditional gene targeting on the pure C57BL/6 genetic background. *Neurosci Res* 58:105–112.
30. Yamasaki M, et al. (2011) Glutamate receptor δ2 is essential for input pathway-dependent regulation of synaptic AMPAR contents in cerebellar Purkinje cells. *J Neurosci* 31:3362–3374.
31. Kitamura K, Judkewitz B, Kano M, Denk W, Häusser M (2008) Targeted patch-clamp recordings and single-cell electroporation of unlabeled neurons *in vivo*. *Nat Methods* 5:61–67.
32. Lonchamp E, et al. (2009) Deletion of $Ca_v2.1(\alpha1_A)$ subunit of Ca^{2+}-channels impairs synaptic GABA and glutamate release in the mouse cerebellar cortex in cultured slices. *Eur J Neurosci* 30:2293–2307.
33. Crepel F, Delhaye-Bouchaud N, Dupont JL (1981) Fate of the multiple innervation of cerebellar Purkinje cells by climbing fibers in immature control, x-irradiated and hypothyroid rats. *Brain Res* 227:59–71.
34. Lohof AM, Delhaye-Bouchaud N, Mariani J (1996) Synapse elimination in the central nervous system: Functional significance and cellular mechanisms. *Rev Neurosci* 7: 85–101.
35. Hashimoto K, et al. (2009) Influence of parallel fiber-Purkinje cell synapse formation on postnatal development of climbing fiber-Purkinje cell synapses in the cerebellum. *Neuroscience* 162:601–611.
36. Altman J (1972) Postnatal development of the cerebellar cortex in the rat. II. Phases in the maturation of Purkinje cells and of the molecular layer. *J Comp Neurol* 145: 399–463.
37. Altman J, Bayer SA (1997) *Development of the Cerebellar System: In Relation to Its Evolution, Structure, and Functions* (CRC, Boca Raton, FL).
38. Kurihara H, et al. (1997) Impaired parallel fiber—>Purkinje cell synapse stabilization during cerebellar development of mutant mice lacking the glutamate receptor δ2 subunit. *J Neurosci* 17:9613–9623.
39. Scelfo B, Strata P (2005) Correlation between multiple climbing fibre regression and parallel fibre response development in the postnatal mouse cerebellum. *Eur J Neurosci* 21:971–978.
40. Goda Y, Davis GW (2003) Mechanisms of synapse assembly and disassembly. *Neuron* 40:243–264.
41. Bosman LW, et al. (2006) Requirement of TrkB for synapse elimination in developing cerebellar Purkinje cells. *Brain Cell Biol* 35:87–101.
42. Ichise T, et al. (2000) mGluR1 in cerebellar Purkinje cells essential for long-term depression, synapse elimination, and motor coordination. *Science* 288:1832–1835.
43. Johnson EM, Craig ET, Yeh HH (2007) TrkB is necessary for pruning at the climbing fibre-Purkinje cell synapse in the developing murine cerebellum. *J Physiol* 582: 629–646.
44. Takagishi Y, et al. (2007) Diminished climbing fiber innervation of Purkinje cells in the cerebellum of myosin Va mutant mice and rats. *Dev Neurobiol* 67:909–923.
45. Ohtsuki G, Hirano T (2008) Bidirectional plasticity at developing climbing fiber-Purkinje neuron synapses. *Eur J Neurosci* 28:2393–2400.
46. Miyazaki T, Watanabe M (2011) Development of an anatomical technique for visualizing the mode of climbing fiber innervation in Purkinje cells and its application to mutant mice lacking GluRδ2 and $Ca_v2.1$. *Anat Sci Int* 86:10–18.